

Case Report

Clear cell sarcoma of soft tissue with multiple cutaneous and subcutaneous metastases resembling plasma cell myeloma: a case study and literature review

Lin Li^{1*}, Chun-Wei Xu^{2*}, Hong Wang³, Yong-Fang Wu², Ge Shen⁴, Bo Zhang², Shu-Ting Huang⁵

Departments of ¹Oncology, ²Pathology, ³Medicine-Cardiovascular, ⁴Radiotherapy, Affiliated Hospital of Academy of Military Medical Sciences, Beijing 100071, P. R. China; ⁵LBP Medicine Science and Technology Co. Ltd., Guangzhou 510663, Guangdong, P. R. China. *Equal contributors.

Received October 24, 2015; Accepted December 23, 2015; Epub February 1, 2016; Published February 15, 2016

Abstract: Clear cell sarcoma of soft tissue is a rare malignancy with low incidence and poor prognosis. We report the case of a 20-year-old male patient with a tumor measuring approximately 14 cm in the right anterior axillary region. Small-round-cell tumor was diagnosed based on needle biopsy in combination with immunohistochemical (IHC) analysis. Solitary plasmacytoma was considered after excluding metastasis to other parts and the tumor was removed by surgical resection. Postoperative pathological investigations indicated clear cell sarcoma of soft tissue: IHC results were positive for vimentin; fluorescence in situ hybridization showed the chromosomal translocation of EWSR1 (22q12) not associated with SS18 (18q11.2), which was characteristic of CCS-ST. Owing to invasion of the muscle and fascia, the tumor could not be completely resected, therefore postoperative radiotherapy to the tumor bed region was applied followed by positron emission tomography: multiple subcutaneous nodules were observed leading to a diagnosis of malignant tumor by biopsy. Drug sensitivity and gene tests suggested that drugs considered effective against sarcoma may be the most beneficial in this case. Therefore the patient underwent a series of different chemotherapy regimens (temozolomide, cyclophosphamide, anthracycline and nab-paclitaxel) plus targeted drugs (sorafenib, bevacizumab, Keytruda, and everolimus). However, remission periods were limited (<10 days) and the tumor grew rapidly exhibiting high malignancy. The patient was finally diagnosed with CCS-ST and died of malignant consumption and extensive progression of tumor with serious infection eight months after surgery. This case report may assist future diagnoses and direct treatment options for CCS-ST.

Keywords: Clear cell sarcoma of soft tissue, melanoma, metastases, chemotherapy, targeted therapy

Introduction

Clear cell sarcoma of soft tissue (CCS-ST) is a rare malignancy that accounts for approximately 1% of all soft tissue sarcomas. Reports on CCS-ST are scarce due to its low incidence worldwide. CCS-ST is primarily observed in young to middle-aged adults, with a peak incidence between 30 and 40 years old, and is more common in females than in males. It mainly occurs in deep soft tissues of distal extremities adjacent to tendons and aponeurosis, especially in the foot and ankle, and to a lesser extent in the trunk; CCS-ST is rarely observed in other parts of the body. Due to its insidious onset and slow growth, CCS-ST is often presented late and has a propensity for metastasis and recurrence. Consequently,

patients with CCS-ST have poor prognosis and the 5-year survival rate is reported to be <50%.

Melanoma of soft tissue (MM-ST) is characterized by the presence of melanin granules in the tumor cells. However, it is histologically distinct from CCS-CT with different prognostic factors. As such, MM-ST requires different treatment regimens.

Here, we report a case of a patient with CCS-ST with multiple cutaneous and subcutaneous metastases resembling plasma cell myeloma (PCM). Based on an in-depth and systematic discussion of his clinicopathological features, we have proposed strategies for more accurate and timely diagnoses and treatment plans in the future.

CCS-ST with multiple cutaneous and subcutaneous metastases: a case study

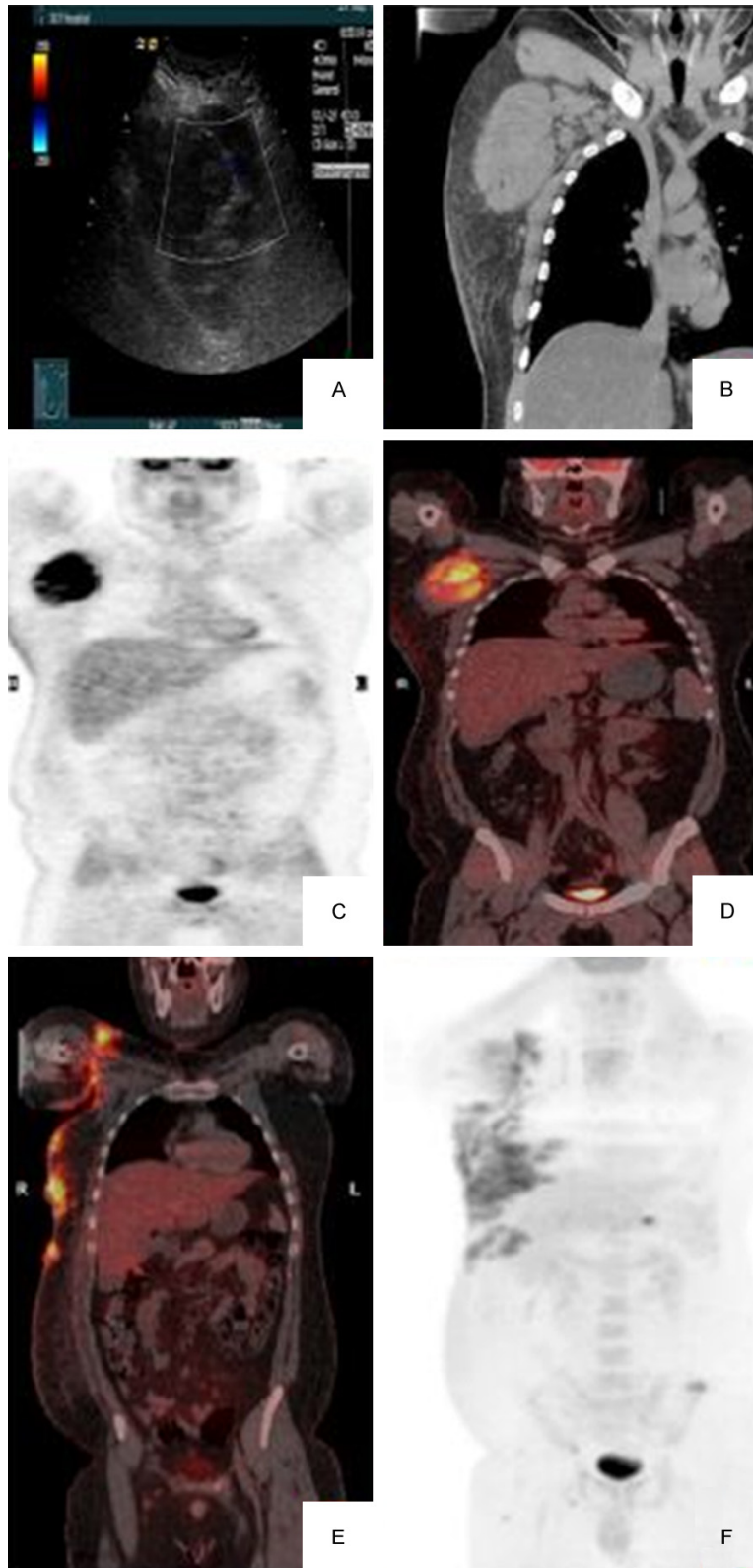


Figure 1. Ultrasonography, chest CT scan and PET-CT examinations during different stages of disease development. (A) Preoperative ultrasound before

surgery: Right axillary near anterior axillary region showed a low echoic solid space occupying lesion, measuring approximately about the size of $10.1 \times 7.6 \times 8.6$ cm. This lesion had an (like for a plurality of fuse into larger range), because the measured value was only for reference, irregular shape with an ill-defined in shape, border was not clear, surrounded by a small volume of fluid visible within a little liquid dark area, large ($2.3 \times 1.6 \times 3.1$ cm). Color Doppler view showed some flow within the lesion, CDV see a little flood flow signals, see (A). (B) Preoperative chest CT scan. 3D reconstruction of the r before surgery Right axillary mass 3D reconstruction showed right axillary multiple and irregular 10.1×8.6 cm following soft tissue masses, irregular shape, with a surrounding fat layer of fat that was visible as a fuzzy, visible strip low density, see (B) layer. (C, D) Preoperative PET MIP and PET-CT scans. before surgery Axillary multiple inhomogeneous nodular masses that had slightly increased or increased radioactive uptake s, with nodular masses, SUVmax 10.7, partial fusion conglomeration unclear boundaries, larger $9.6 \text{ cm} \times 8.3 \text{ cm}$, no abnormal uptake in other parts, right chest wall subcutaneous edema was evident. The scans were consistent with a malignant neoplasm (C+D). (E, F) PET-CT scans before the fourth cycle of chemotherapy and molecular targeting treatment. The right-sided lower neck, right subclavian, right internal mammary area, right upper arm, chest and abdominal wall, back, hips, right groin, and the right lower limb the proximal muscle showed, multiple subcutaneous, multiple soft tissue thickening or nodules (SUVmax 12.4). There was a diffuse, non-uniform increase in uptake in the, head, trunk, and multiple sites within the bone and bone marrow uptake diffuse non-uniform increased, (SUVmax 3.7). CT images shown focal bone destruction. On the right- sided of ilium, right sacrum, right pubis and right acetabulum (E+F).

CCS-ST with multiple cutaneous and subcutaneous metastases: a case study

Table 1. Primary antibodies used for immunohistochemical staining

Antibody	Clone	Dilution	Corporation purchased from
CK	AE1/AE3	1:100	Zymed Laboratories, Inc.
Vimentin	EP21	1:100	Zymed Laboratories, Inc.
EMA	GP1.4	1:100	Zymed Laboratories, Inc.
Syn	EP158	1:100	Zymed Laboratories, Inc.
CgA	EP38	1:100	Zymed Laboratories, Inc.
S-100	15E2E2+4C4.9	1:100	Zymed Laboratories, Inc.
Desmin	EP15	1:100	Zymed Laboratories, Inc.
Melanoma-pan	HMB45	1:100	Zymed Laboratories, Inc.
Melan A	A103	1:100	Zymed Laboratories, Inc.
D2-40	D2-40	1:100	Zymed Laboratories, Inc.
Bcl-2	EP36	1:100	Zymed Laboratories, Inc.
Bcl-6	LN22	1:100	Zymed Laboratories, Inc.
CyclinD1	EP12	1:100	Zymed Laboratories, Inc.
CD3	EP41	1:100	Zymed Laboratories, Inc.
CD5	EP77	1:100	Zymed Laboratories, Inc.
CD10	EP195	1:100	Zymed Laboratories, Inc.
CD20	EP7	1:100	Zymed Laboratories, Inc.
CD21	EP64	1:100	Zymed Laboratories, Inc.
CD23	EP75	1:100	Zymed Laboratories, Inc.
CD30	EP154	1:100	Zymed Laboratories, Inc.
CD38	SPC32	1:100	Zymed Laboratories, Inc.
CD56	UMAB83	1:100	Zymed Laboratories, Inc.
CD79 α	EP82	1:100	Zymed Laboratories, Inc.
CD99	EP8	1:100	Zymed Laboratories, Inc.
CD117	EP10	1:100	Zymed Laboratories, Inc.
CD138	MI15	1:100	Zymed Laboratories, Inc.
WT-1	EP120	1:100	Zymed Laboratories, Inc.
MUM-1	EP190	1:100	Zymed Laboratories, Inc.
LCA	RP2/18+RP2/22	1:100	Zymed Laboratories, Inc.
PAX-5	EP156	1:100	Zymed Laboratories, Inc.
Kappa	EP171	1:100	Zymed Laboratories, Inc.
Lambda	EP172	1:100	Zymed Laboratories, Inc.
TdT	SEN28	1:100	Zymed Laboratories, Inc.
PLAP	EP194	1:100	Zymed Laboratories, Inc.
Ki-67	EP5	1:100	Zymed Laboratories, Inc.

Case report

The patient was a 20-year-old man with obesity (weight, 120 kg) and a history of smoking (10 years). He was admitted to our hospital on September 25, 2014 for three weeks after presenting with a right axillary mass with symptoms of redness, swelling, heat and pain following trauma in early September, 2014. The mass was approximately 10 × 6 cm, fixed, with no clear border and a maximum body temperature of 38.9°C. When questioned about its medical

history, the patient reported that he had accidentally palpated the mass two years ago at which time it measured approximately 3 cm but he had not presented it. He was given intravenous infusion of cefazolin for one week. Although the swelling and fever were relieved, the mass was still palpable.

On September 10, 2014, an ultrasound examination revealed a solid mass in the right anterior axillary region, approximately 10.1 × 7.6 × 8.6 cm in size. The mass was irregular in shape resembling multiple nodes and had no clear border. The scan also showed a small area of dark liquid within the mass, measuring approximately 2.3 × 1.6 × 3.1 cm (**Figure 1A** and **1B**). Pathological examination by biopsy indicated plasma cell neoplasm; subsequent gross section pathological consultation at the Cancer Hospital of Chinese Academy of Medical Sciences suggested atypical small-round-cell tumor (SRCT) of the lymphatic/hematopoietic systems. A subsequent pathological consultation at the Beijing Cancer Hospital also suggested SRCT, most probably plasma cell tumor. Immunohistochemical (IHC) analysis gave the following results:

Cyclin D1 (diffuse+), CD138 (+), MUM-1 (+), CD38 (-), CD10 (-), CD20 (-), CD21 (-), CD3 (T+), CD79 α (-), Kappa (weak+), Lambda (-), CD117 (-), Ki67 (~80%) (**Table 1**). On September 18, 2014, positron emission tomography (PET) showed increased or slightly increased radioactive uptake in the right axilla (SUVmax = 10.7), with multiple inhomogeneous nodular masses and a partially fused conglomeration approximately 9.6 × 8.3 cm in size. The mass was considered to be malignant. No abnormal metabolic activity was observed in the bilateral neck,

CCS-ST with multiple cutaneous and subcutaneous metastases: a case study

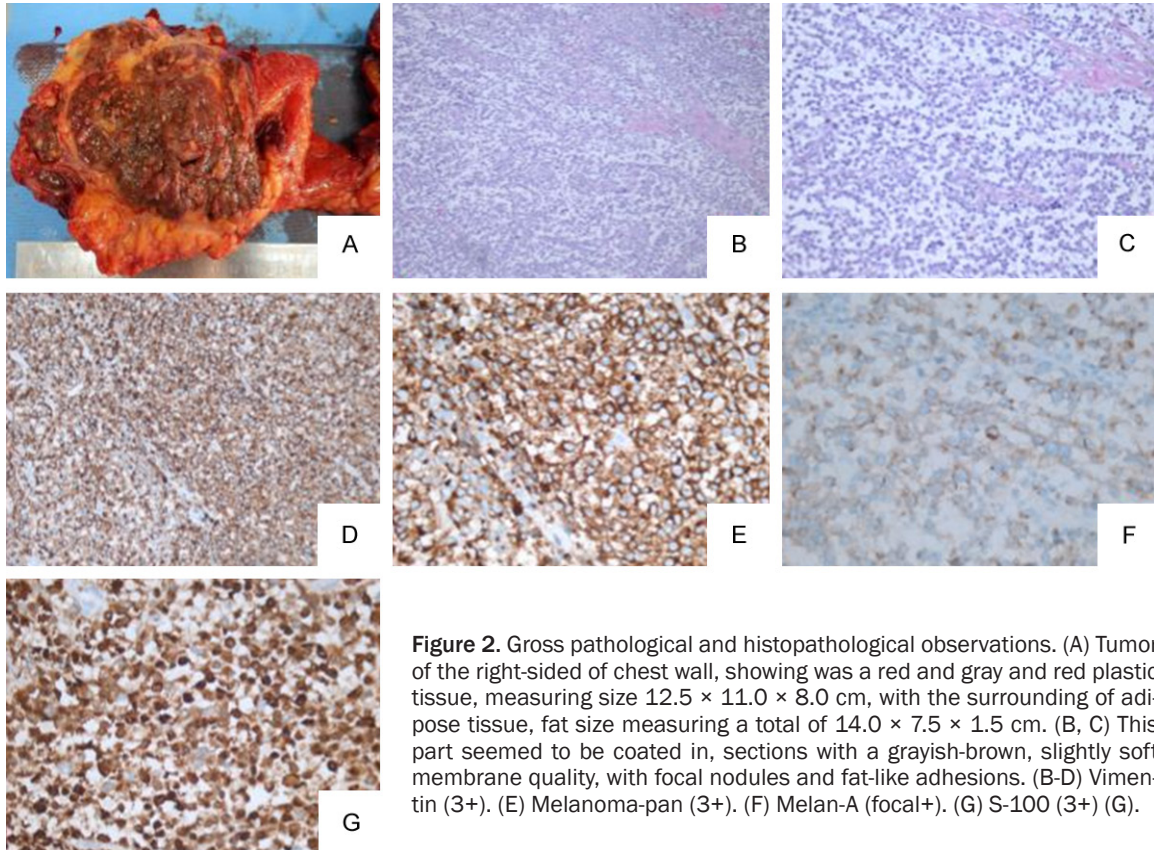


Figure 2. Gross pathological and histopathological observations. (A) Tumor of the right-sided of chest wall, showing was a red and gray and red plastic tissue, measuring size 12.5 × 11.0 × 8.0 cm, with the surrounding of adipose tissue, fat size measuring a total of 14.0 × 7.5 × 1.5 cm. (B, C) This part seemed to be coated in, sections with a grayish-brown, slightly soft membrane quality, with focal nodules and fat-like adhesions. (B-D) Vimentin (3+). (E) Melanoma-pan (3+). (F) Melan-A (focal+). (G) S-100 (3+) (G).

supraclavicular or left axillary regions or in any other part of the body (**Figure 1C** and **1D**); furthermore, the patient had no anemia and was negative for Bence Jones protein. Other blood indices were as follows: serum albumin, 47.4 g/L; globulin, 43 g/L; protein electrophoresis, α_1 15.2%, α_2 13.3%, β_1 6.7%, β_2 8.8% and γ 18.6%; IgA, 6.60 g/L; uric acid, 578 μ mol/L; with no abnormal immunoglobulin κ and λ light chains.

Based on his clinical manifestations, imaging features and biopsy pathologies, the patient was diagnosed with solitary plasmacytoma. Resection of the right axillary tumor was performed on September 30, 2014. Intraoperative exploration showed a hard, fixed, irregular mass approximately 15 × 16 cm in size, at the third to fifth intercostal axillary midline in the right chest wall; the upper boundary reached the axilla with no clear medial boundary from the chest wall muscle; the back boundary reached the posterior axillary line. The tumor infiltrated the long thoracic and thoracodorsal nerves and compressed the axillary vein and wall plexus branches.

Resection of the tumor was carried out and the tissue was submitted for postoperative gross pathology. The tumor measured 12.5 × 11.0 × 8.0 cm and the surrounding adipose tissue measured 14.0 × 7.5 × 1.5 cm. The tissue from the right side of chest wall was plastic and grayish-red in color. Part of the mass was capsulated with a slightly soft texture and a grayish-brown cross-section. The nodular focal lesion appeared to be adhered to the fat. IHC analyses at several hospitals gave the following results: Vimentin (3+), Bcl-2 (3+), CyclinD1 (3+), Bcl-6 (focal+), CK (focal+), CD138 (+), MUM-1 (+), CD38 (-), CD99 (-), WT-1 (-), LCA (-), CD20 (-), PAX-5 (-), CD79 α (-), Kappa (-), Lambda (-), CD30 (-), CD23 (-), CD5 (-), CD56 (weak+), TdT (-), PLAP (-), CD117 (-), EMA (-), Syn (-), CgA (-), D2-40 (-), Ki-67 (80%), S-100 (3+), Melanoma-pan (3+), Melan-A (focal+) and Desmin (-) (**Figure 2A-G**; **Table 1**). Fluorescence in situ hybridization (FISH) analysis of the tumor cells showed separation in the EWSR1 signals with no separation of SS18 signals, indicating chromosomal translocation of EWSR1 (22q12) not associated with SS18 (18q11.2) (**Figure 3**). Based on these data, the patient was diagnosed with CCS-ST.

CCS-ST with multiple cutaneous and subcutaneous metastases: a case study

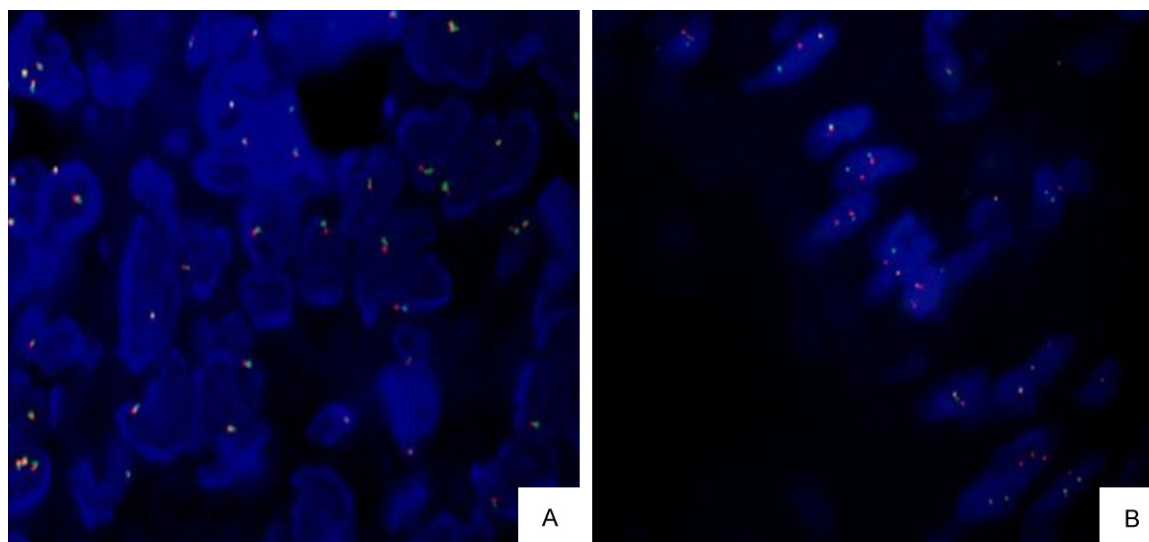


Figure 3. A. EWSR1 (22q12) translocation; B. SS18 (18q11.2) no-translocation.

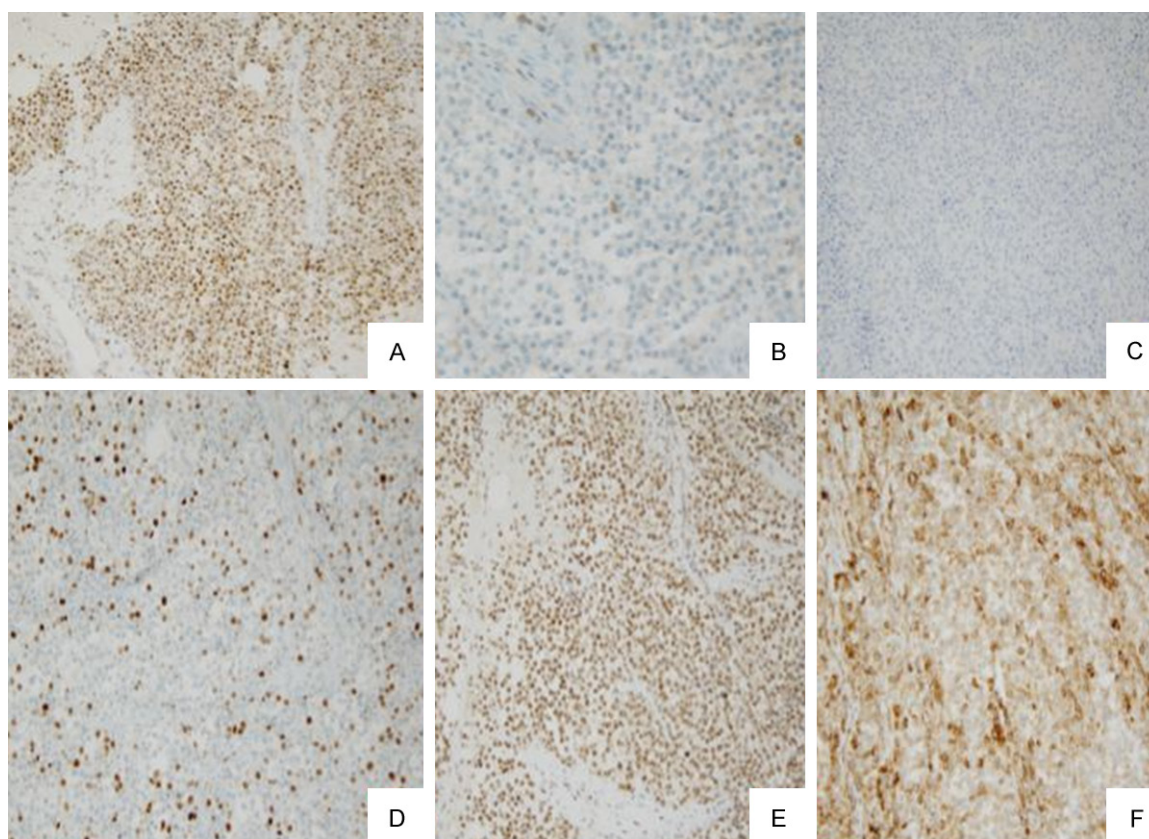


Figure 4. Immunohistochemical staining for the expression of MGMT, PD-1, PGP, TOP2A, TOP1 and TUBB3: (A) MGMT 20 × (+) (A); (B) PD-1 40 × (+) (B); (C) PGP 20 × (-) (C); (D) TOP2A 20 × (+); (E) TOP1 20 × (+); (F) TUBB3 20 × (-).

Due to tumor invasion of the muscle and fascia, complete resection had not been possible; therefore radiotherapy to the tumor bed was

administered from October 27, 2014. Multiple subcutaneous nodules with symptoms of pain and swelling were observed when the dose

CCS-ST with multiple cutaneous and subcutaneous metastases: a case study

Table 2. Gene mutations without notable results identified by next-generation sequencing of the patient

Gene	Type	Gene	Type
ABL1	Wild type	KDR (VEGFR2)	Wild type
AKT1	Wild type	KRAS	Wild type
ALK	Wild type	MPL	Wild type
APC	Wild type	NOTCH1	Wild type
ATM	Indeterminate	NPM1	Wild type
BRAF	Wild type	NRAS	Wild type
BRCA1	Wild type	PDGFRA	Wild type
BRCA2	Wild type	PIK3CA	Wild type
CDH1	Wild type	PTEN	Wild type
c-KIT	Wild type	PTPN11	Wild type
c-MET	Wild type	RB1	Wild type
CSF1R	Wild type	RET	Wild type
CTNNB1	Wild type	SMAD4	Wild type
EGFR	Wild type	SMARCB1	Wild type
ERBB4	Wild type	SMO	Indeterminate
FBXW7	Wild type	STK11	Wild type
FGFR1	Wild type	TP53	Wild type
FGFR2	Wild type	VHL	Wild type
FLT3	Wild type	HNF1A	Wild type
GNA11	Wild type	HRAS	Wild type
GNAQ	Wild type	IDH1	Wild type
GNAS	Wild type	JAK2	Wild type
Her2/Neu (ERBB2)	Wild type	JAK3	Wild type

reached 95%PTV56Gy/28F. On December 9, 2014, PET-CT examination revealed a mass occupying the right axillary surgical area adhered to the tissue of the adjacent muscle. The mass was metabolically active and considered to have developed from residual tumor tissue. Multiple subcutaneous metastatic nodules were observed in the right axillary region, right shoulder, right arm and torso; multiple metastatic nodules had developed in the right anterior serratus muscle, right latissimus dorsi muscle and right teres minor; hypermetabolic small lymph nodes had metastasized in the right internal mammary area (**Figure 1E** and **1F**); and malignant tumor infiltration was observed in the deep dermis and subcutaneous tissue. A subcutaneous nodule, approximately 0.6 × 0.5 × 0.5 cm in size, was resected from the right side of waist for pathological examination. The results, combined with the preceding observations and patient's medical history, indicated metastases of CCS-ST. Therefore, one cycle of chemotherapy with temozolomide plus bevacizumab and sorafenib was administered from December 9, 2014.

After 1-5 days of chemotherapy the subcutaneous nodules had significantly reduced, however they then rapidly increased in both number and size (**Figure 5A**).

A drug sensitivity test was performed on the gross tumor specimens. Second-generation gene sequencing showed that KRAS, NRAS, PDGFR and BRAF existed as wild-type genes in the tumor. In combination, these results suggested that the most beneficial drugs would be those considered effective against sarcoma (**Figure 4; Table 2**). The treatment regimen was therefore changed to three cycles of chemotherapy with epirubicin combined with ifosfamide, etoposide, plus bevacizumab on January 8, 2015. Although the subcutaneous nodules significantly reduced within 10 days of each cycle, they then grew rapidly in size and number and multiple nodules exhibited ulceration and discharge, limiting the patient's daily activity.

On March 24, 2015, a PET-CT scan showed multiple subcutaneous and bone metastases; therefore the treatment regimen was revised to chemotherapy with nab-paclitaxel plus bevacizumab, sorafenib, Keytruda (anti-programmed death 1 monoclonal antibody) and everolimus. However, the subcutaneous nodules continued to progressively increase in size and number as before (**Figure 5B**). Furthermore, systemic multiple subcutaneous nodules showed ulceration and discharge with an unpleasant smell; decreased albumin was also recorded. The general condition of patient gradually deteriorated and he eventually died of extensive tumor progression, malignant consumption and serious infection eight months after surgery. Details of the treatment history are summarized in **Table 3**.

Discussion

CCS-ST originates from the neuroectoderm and was first reported by Enzinger in 1965 [1]. In 1983, Chung et al. proposed the term MM-ST to describe those tumors containing melanin in the cells [2]. This classification was further divided into a melanin or synovial subtype by

CCS-ST with multiple cutaneous and subcutaneous metastases: a case study



Figure 5. The gross tumor picture at different course of disease development. A. Early disease recurrence early; B. After four cycles of chemotherapy and molecular targeted treatment.

Table 3. Details of the treatment process

Date	Regimen	Drug	Dosage	Administration
12 th Sep 2014	Biopsy			
30 th Sep 2014	Surgery			
27 th Oct 2014	IMRT			
9 th Dec 2014	TBS (1 Cycle)	Temozolomide Bevacizumab Solafinib*	400 mg 600 mg 800 mg	p.o. qd i.v. p.o. bid D1-5 D1, D14 D1-D28
15 th Jan 2015	ELE (2 Cycle)	Epirubicin Ifosfamide Etoposide	70 mg 2 g 100 mg	i.v. i.v. i.v. D1-D2 D1-D3 D1-D5
28 th Feb 2015	CAV (1 Cycle)	Adriamycin Vincristine Cyclophosphamide	170 mg 2 mg 2.8 g	i.v. i.v. i.v. D1 D1 D1
24 th Mar 2015	PBSP (2 Cycle)	Nab-Paclitaxel Bevacizumab Solafinib* Keytruda	500 mg/300 mg 600 mg 400 mg 250 mg	i.v. i.v. p.o. bid i.v. D1, D29 D1, D14 D1-D28 D24
12 th May 2015		everolimus Keytruda	10 mg 250 mg	p.o. qd i.v. D1-D10 D1

i.v., intravenous; po, orally; D, day. *Did not complete for toxicity. Treatment parameters: height 178 cm, weight 120 kg, BSA: 2.36 m².

Tsuneyoshi et al. in 1978 [3]. Approximately half of all patients with CCS-ST have a history of trauma, resulting in a hard mass localized within the tissue with symptoms of swelling, pain and tenderness. To date, no consensus on an effective systematic treatment for CCS-ST has been reached. Moreover, poor understanding of its clinical behavior has led to misdiagnoses in many cases affecting treatment outcomes.

Gross specimens of CCS-ST are spherical or nodular with a grayish-white fish-like appearance. A brown or black substance is visible in 20%-25% of specimens. In the absence of a clear capsule, the tumor readily invades surrounding tissue to form a pseudocapsule occasionally showing focal necrosis and has a tendency to undergo early regional lymph node metastases, with relatively more pulmonary

CCS-ST with multiple cutaneous and subcutaneous metastases: a case study

metastases compared to other soft tissue sarcomas [4]. Some cases of CCS-ST exhibit pulmonary and lymph node metastasis simultaneously. As such, regular inspection of the lung is recommended, in addition to CT or MRI examination of lymph node metastasis in the axillary, abdominal, and pelvic regions.

The size and depth of a tumor are two of the most important predictors of distant metastasis and survival in CCS-ST. Early diagnosis of CCS-ST and timely extensive resection of tumors <5 cm can improve the prognosis of patients with CCS-ST. However, in cases presenting tumors >5 cm or deep-seated tumors, effective chemotherapy regimens remain to be established. As such, treatment strategies for CCS-ST favor those for sarcoma over those for cutaneous melanoma.

The following pathological and morphological examinations can facilitate an accurate diagnosis of CCS-CT or MM-ST: CT examination typically shows a tumor with no clear boundary in close proximity to tendons, muscle membranes or fascia. It rarely invades the skin, bone or surrounding tissue; however, in a small number of cases the primary metastatic site originates in the bone. Magnetic resonance imaging (MRI) scans of CCS-ST are characterized by equal intensity T1 signals with high T2 signals, partially mixed with low T1 and high T2 signals. IHC analysis has shown that CCS-ST cells are positive for vimentin, HMB45, S-100 and PAS staining [5-7]. Molecular genetic characterization has confirmed that ectopic chromosome t(12, 22)(q13, Q12) is specific to CCS-ST and that this feature is distinct from cutaneous MM. Conversely, BRAF mutations only occur in cutaneous MM. CCS specifically expresses the EWS/ATF1 fusion gene, therefore different fracture sites of the fusion gene may be a prognostic factor for CCS-ST; whereas a mutation in the BRAF gene has implications for differential diagnosis between CCS and unclear MM in the primary site. Although they exhibit similar histological compositions, CCS-ST and MM-ST are independent tumor entities [8-11]. In addition, the clinical behavior of CCS-ST is closer to that of soft tissue carcinomas than cutaneous melanoma despite sharing similar tissue origins and a high incidence of local recurrence.

In summary, the key pathological diagnostic criteria for CCS-ST and MM-ST are as follows: 1)

relatively uniform round or oval shape; 2) large and clear nucleoli with rare mitotic figures; 3) a fiber matrix composed of reticular cords; 4) no diphasic differentiation; 5) and diffuse multinucleated giant cells. In addition, electron microscopy shows melanin-like pigments and melanin at different stages.

This patient in this case was atypical. He was admitted with multiple cutaneous and subcutaneous metastases and multiple bone metastases. Based on preoperative biopsy and postoperative pathological investigations along with consultations at multiple hospitals, he was initially diagnosed with PCM or malignant SRCT. The patient subsequently underwent a series of treatment regimens for sarcoma and melanoma, each of which involved different chemotherapy and targeted drugs. However these all failed. He was eventually diagnosed with CCS-ST more than one month after surgery and died after eight months after surgery.

Various combinations of chemotherapeutic and targeted were administered, however remission periods remained low and the tumor continued to grow rapidly. The different treatment regimens and the results of the corresponding examinations were as follows: Preoperative PET-CT scans excluded distant lesions, especially multiple osteolytic lesions; blood immunoglobulin fixation electrophoresis found no specific immune precipitation; and Bence Jones protein was not detected in urine examination. Solitary PCM was diagnosed and the patient underwent surgical resection of the tumor tissue. However, the disease progressed rapidly and multiple subcutaneous metastases occurred during tumor bed irradiation for residual lesions. Postoperative pathology, including specific IHC and FISH examinations of the tumor tissue, along with drug sensitivity and gene testing, finally led to the patient being diagnosed with CCS-ST.

The results from these investigations suggested that the tumor may be sensitive to adriamycin, nab-paclitaxel and Keytruda. Keytruda was the newest drug and has shown good efficacy in the treatment of melanoma. The first cycle of chemotherapy involved two molecular targeted drugs (sorafenib and bevacizumab) combined with temozolomide. This was subsequently followed with three cycles of chemotherapy with adriamycin and etoposide combined with cyclo-

phosphamide. Finally, the treatment regimen was changed to nab-paclitaxel plus bevacizumab, sorafenib and Keytruda. Although the subcutaneous nodules were slightly reduced following this final treatment, the remission period was less than 10 days.

This case study demonstrated the importance of excluding malignant CCS-ST prior to a diagnosis of SRCT. More data are required to ensure that the most effective systemic chemotherapy and molecular targeted therapies for CCS-ST and MM-ST are adopted in future, and whether these should favor those for sarcoma or targeted therapies including immune therapy.

Disclosure of conflict of interest

None.

Address correspondence to: Dr. Lin Li, Department of Oncology, Affiliated Hospital Cancer Center, Academy of Military Medical Sciences, 8 Dongda Street, Fengtai District, Beijing 100071, P. R. China. Tel: 86 +10-66947177; Fax: 86 +10-66947177; E-mail: linli010120@163.com

References

- [1] Enzinger FM. Clear-cell sarcoma of tendons and aponeuroses. An analysis of 21 cases. *Cancer* 1965; 18: 1163-74.
- [2] Chung EB, Enzinger FM. Malignant melanoma of soft parts. A reassessment of clear cell sarcoma. *Am J Surg Pathol* 1983; 7: 405-413.
- [3] Tsuneyoshi M, Enjoji M, Kubo T. Clear cell sarcoma of tendons and aponeuroses. A comparative study of 13 cases with a provisional subgrouping into the melanotic and synovial types. *Cancer* 1978; 42: 243-252.
- [4] Lucas DR, Kshirsagar MP, Biermann JS, Hamre MR, Thomas DG, Schuetze SM, Baker LH. Histological alterations from neoadjuvant chemotherapy in high-grade extremity soft tissue sarcoma: clinicopathological correlation. *Oncologist* 2008; 13: 451-8.
- [5] Quesada J, Amato R. The Molecular Biology of Soft-Tissue Sarcomas and Current Trends in Therapy. *Sarcoma* 2012; 2012: 849456.
- [6] Husain N, Verma N. Current Concepts in Pathology of Soft Tissue Sarcoma. *Indian J Surg Oncol* 2011; 2: 302-308.
- [7] Curry CV, Dishop MK, Hicks MJ, Naeem R, Reed JA, Lopez-Terrada DH. Clear cell sarcoma of soft tissue: diagnostic utility of fluorescence in situ hybridization and reverse transcriptase polymerase chain reaction. *J Cutan Pathol* 2008; 35: 411-417.
- [8] Hisaoka M, Ishida T, Kuo TT, Matsuyama A, Imamura T, Nishida K, Kuroda H, Inayama Y, Oshiro H, Kobayashi H, Nakajima T, Fukuda T, Ae K, Hashimoto H. Clear cell sarcoma of soft tissue: a clinicopathologic, immunohistochemical, and molecular analysis of 33 cases. *Am J Surg Pathol* 2008; 32: 452-460.
- [9] Hocar O, Le Cesne A, Berissi S, Terrier P, Bonvalot S, Vanel D, Auperin A, Le Pechoux C, Bui B, Coindre JM, Robert C. Clear cell sarcoma (malignant melanoma) of soft parts: a clinicopathologic study of 52 cases. *Dermatol Res Pract* 2012; 2012: 984096.
- [10] Mavrogenis A, Bianchi G, Stavropoulos N, Pappalopoulos P, Ruggieri P. Clinicopathological features, diagnosis and treatment of clear cell sarcoma/melanoma of soft parts. *Hippokratia* 2013; 17: 298-302.
- [11] Kosemehmetoglu K, Folpe AL. Clear cell sarcoma of tendons and aponeuroses, and osteoclast-rich tumour of the gastrointestinal tract with features resembling clear cell sarcoma of soft parts: a review and update. *J Clin Pathol* 2010; 63: 416-423.